

Camera Lidar Observations of Aerosols and Comparisons with Aerosol Optical Depth

Nimmi C. P. Sharma^(a), Amin Kabir^(b), John E. Barnes^(c),

Meg Farinsky^(a), Gabriel E. Garcia^(a), Pablo Escalante^(a), Marcus Alcantara-Silva^(a) and George Odhiambo^(d),

^(a) Central Connecticut State University

Department of Physics and Engineering Physics, 1615 Stanley Street, New Britain, CT 06050 U.S.A.

^(b) University of the Bahamas

Department of Physical and Earth Sciences, University Drive, Nassau, The Bahamas

^(c) National Oceanic and Atmospheric Administration (NOAA) Global Monitoring Laboratory
325 Broadway R/GML, Boulder CO 80305-3328 U.S.A.

^(d) University of the Bahamas

School of Chemistry Environment and Life Sciences, University Drive, Nassau, The Bahamas

Nimmi Sharma e-mail address: sharmanim@ccsu.edu

Abstract: A bistatic atmospheric camera lidar system consisting of a vertically transmitted continuous wave laser and a distantly located CCD camera detector is used to observe atmospheric aerosols by measuring the nighttime laser light scattering. The detector, consisting of a CCD camera fitted with wide angle optics and a laser line filter, images the entire transmitted laser beam from the side. The brightness at each pixel provides the side-scattered signal, and the altitude of the scatterer is determined from geometry rather than timing. As with traditional lidar, the signal is normalized to a molecular model at high altitudes and is transmission corrected. Side-scatter is converted to total scatter using an aerosol scattering phase function derived from AERONET data at the nearest available AERONET site. Aerosol extinction is calculated and integrated to derive aerosol optical depth. Results are compared to NASA MERRA2 and AERONET aerosol optical depth data.

1. Introduction

Aerosol detection and monitoring is important for a host of atmospheric studies. Aerosols influence air quality and human health. They impact precipitation patterns. Aerosols affect climate. In addition, entrained aerosols can serve as tracers to elucidate large scale atmospheric transport phenomena. Lidar has proved a useful tool for studying the spatial and temporal distributions of aerosols.

Traditional ground-based backscatter atmospheric lidar systems are typically monostatic systems which employ pulsed laser transmitters with detectors located at the same site as the transmitter. In these systems, scattered laser light from air molecules, clouds and suspended particulates (aerosols) is measured and the altitude of the scatterer is determined by measuring the time from the pulse transmission to the detection of the scattered photons. While these systems offer valuable data for many studies [1][2][3], their

widespread use has been limited by constraints including expense, field ruggedness, and system temperature regulation requirements. For near ground measurements, traditional systems also face field of view overlap issues. The bistatic camera lidar system employed in this study is a rugged, inexpensive system capable of providing data at low altitudes without overlap issues [4][5][6].

2. Camera Lidar

The CCD Camera Lidar in this study uses a bistatic configuration where the detector is spatially separated from the transmitter. The transmitter consists of a 5 W Continuous wave solid state 532 nm green laser mounted vertically on a tripod. A quarter waveplate mounted at the transmitter changes the laser polarization to circular polarization to mimic unpolarized light over the timeframe of the detector exposure. The laser is transmitted vertically into the atmosphere. The detector is located a substantial distance, D , from the

transmitter. The detector consists of a CCD camera with a 10 nm wide laser line interference filter and a wide-angle lens that allows for imaging the entire laser beam from ground to zenith simultaneously on the CCD chip. Each pixel images a portion of the beam at scattering angle Θ with angular size $d\Theta$. This yields a varying altitude resolution, with sub-meter resolution at altitudes near the ground and coarser altitude resolution at higher altitudes. The system operates only at night.

The camera exposures produce a data image in which the brightness of the laser beam shows the combined side scatter from air molecules, aerosols and clouds. Unlike in traditional lidar, where all altitudes have the same scattering angle (180 degrees), the Camera Lidar has different scattering angles for different altitudes. The altitude of the scatterers can be determined from the site location geometry and does not require timing, allowing for the use of a rugged and inexpensive CW laser as the transmitter. The varying altitude resolution cancels out the typical range squared dependence of the signal as the length of the beam imaged in each pixel grows with altitude. Figure 1 shows the Camera Lidar geometry.

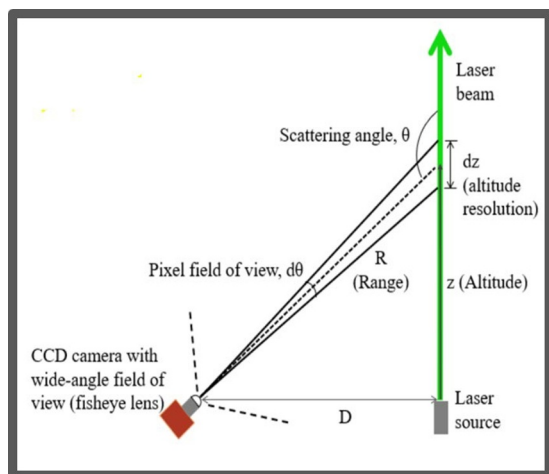


Figure 1: Camera Lidar Geometry

3. Experimental Procedure

In this study, a Camera Lidar system was used to observe aerosols at University of the Bahamas in a darkened field at Nassau, Bahamas (25.06N, 77.36W). The camera detection system was located 91.5 m from the laser. Exposures were taken after sunset on January 12, 2023. Each exposure was 120 seconds long. Figure 2 shows a raw data image from the experiment. The beam is placed

diagonally on the CCD chip to allow imaging from ground to zenith.

Captured images are analyzed to quantify the beam brightness at each altitude. First the beam is detected. Then a Gaussian plus a constant is fit across the beam at each altitude. The constant yields the background and the area under the Gaussian yields the signal.



Figure 2: Data Image from Camera Lidar

As with traditional lidar, the signal is normalized to a molecular model in a normalization range which is assumed to be aerosol-free. The molecular model for this experimental site was constructed by combining five years of local radiosonde measurements at lower altitudes with the U.S. Naval Research Lab MSIS model [7] at higher altitudes. For this study the normalization altitude range was 5 to 9 km. The model is matched to the signal in this region where scattering is assumed to be purely molecular, to allow the molecular component of the scattering to be subtracted from the signal. Following normalization, the data are corrected for transmission.

To convert aerosol side scatter at each altitude to aerosol total scatter so aerosol extinction and optical depth can be derived, an aerosol scattering phase function, representing the scattering efficiency into each angle, is required because each altitude has a different scattering angle in the bistatic Camera Lidar configuration. In this study, the aerosol scattering phase function used was derived from solar radiation measurements taken by

NASA's Aerosol Robotic Network, AERONET [8], at Key Biscayne, Florida, U.S.A, (25.7N, 80.2W) the nearest available AERONET site to our experimental site. As AERONET data are acquired during the day at specific wavelengths and the Camera Lidar ran at nighttime at 532 nm, the phase function data used are from the day of our evening experiment and are interpolated to our laser wavelength.

With the assumption of a single scattering albedo, aerosol extinction is then derived from the Camera Lidar data. The extinction is then integrated over altitudes up to the normalization range to derive the Camera Lidar Aerosol Optical Depth (AOD). The Camera Lidar AOD is then compared to the daily average AOD from AERONET data at Key Biscayne converted to 532 nm for the date of the experiment. For another perspective, Camera Lidar data were also compared to NASA's Modern-Era Retrospective Research and Analysis version 2, MERRA2, AOD at 550 nm, for the area of the experiment for the hours leading up to the experiment on the experimental date.

4. Results

Figure 3 shows the Camera Lidar Aerosol Extinction averaged over eight exposures of duration two minutes each.

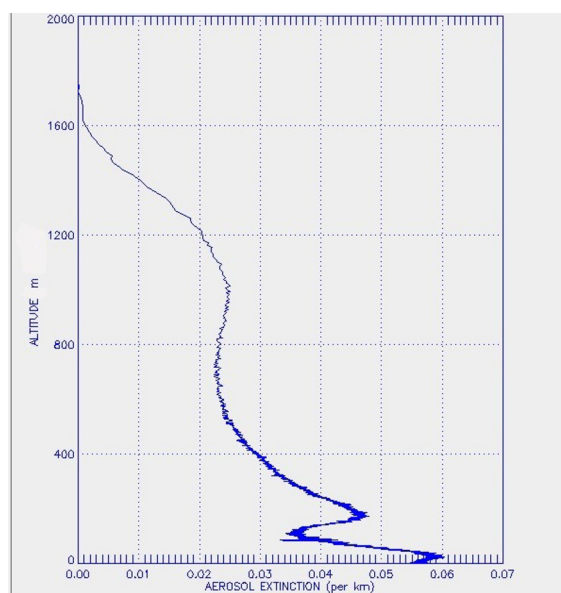


Figure 3: Altitude vs. Average Aerosol Extinction

The variation over time in near ground extinction is shown in Figure 4, in which the

horizontal axis represents the exposure time, the vertical axis represents altitude in pixels along the beam (bin) and in km, and the extinction in Mm^{-1} is represented as a colormap. Note that in Figure 4 the vertical axis is linear in image pixel (bin) and thus nonlinear in km.

Aerosol optical depth from the Camera Lidar measurements was compared to the daily average of the Key Biscayne AERONET AOD. Camera Lidar data at Nassau, Bahamas for the times in this study yielded an average AOD of 0.037. AERONET daily average AOD for the same day at Key Biscayne of 0.043. The Camera Lidar and AERONET AODs showed agreement to within a 15% difference.

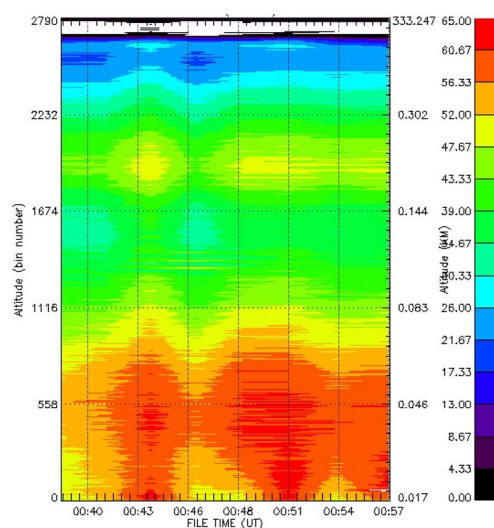


Figure 4: Altitude profile of Aerosol Extinction in Mm^{-1} with time

Camera Lidar AOD was also compared to MERRA2 AOD at 550 nm [9]. Figure 5 shows the MERRA2 data encompassing Key Biscayne and Nassau, Bahamas for the hours before the Camera Lidar experiment.

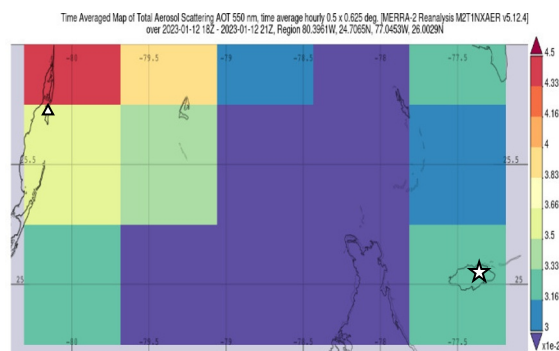


Figure 5: MERRA2 AOT over Key Biscayne (triangle) and Nassau, Bahamas (star).

AOD at Key Biscayne was slightly higher than AOD at Nassau, consistent with the Camera Lidar results. Camera Lidar AOD differed from MERRA2 AOD over the Bahamas by approximately 13 percent.

5. Discussion and Future Work

Experiments to map aerosols vertically in the atmosphere over time were conducted using an inexpensive and rugged bistatic camera lidar system optimized for boundary layer studies. This study demonstrates the ability of Camera Lidar to map aerosols all the way to the ground with excellent near-ground altitude resolution. The system can also aide in visualization of near-ground aerosol variability. Retrieved Camera Lidar AOD showed very good agreement with both AERONET and MERRA2 AOD data.

There are some challenges faced by the Camera Lidar which provide opportunities for future work. The Camera Lidar currently only operates at night due the wide-angle optics which require a wide-band (10 nm bandwidth) laser line interference filter to ensure no loss of signal at the beam ends. Thus, AOD comparisons are made with daytime AOD. However, as can be seen in the Figure 2 data image, the system images stars as well as the laser beam, and thus could also be used as a star photometer to derive nighttime AOD from the data image separately from the laser beam AOD. The need for an aerosol scattering phase function to convert side-scatter to total scatter has been handled by using aerosol phase functions derived from nearby AERONET sites. These represent a column average phase function. Ideally, an on-site polar nephelometer which could directly measure the aerosol phase function at the ground would be desirable. This instrument is currently under development. Another method of deriving the aerosol scattering phase function more directly is to use two camera detectors placed at different distances from the laser. The laser scattering from each altitude would then be imaged simultaneously from two different scattering angles, providing information to constrain the phase function. This work is in progress.

The Camera Lidar offers an inexpensive, capable and field-ready alternative to

traditional lidar systems for observations of atmospheric aerosols, especially in the near-ground region. Derived AOD compares well with satellite and ground-based measurements. Future work to expand the technique offers promise for enhancing system capabilities.

6. References

- [1] Nimmi Sharma, "Laser Radar: A Technique for Studying the Atmosphere," *Resonance* **16**, no. 1, 38-46 (2011).
- [2] N. C. Parikh and J. A. Parikh, "Systematic Tracking of Boundary Layer Aerosols with Laser Radar," *Journal of Optics and Laser Technology*, **34**, no. 2, 177-185, 2002.
- [3] N. C. Parikh and J. A. Parikh, "Visualizing Cloud Patterns with Micro Pulse Lidar," *Proceedings of the 21st International Laser Radar Conference: Lidar Remote Sensing in Atmospheric and Earth Sciences*, 639-642, July 8-12, 2002, Quebec City, Canada.
- [4] John E. Barnes, N. C. Parikh Sharma and Trevor B. Kaplan, "Atmospheric aerosol profiling with a bistatic imaging lidar system", *Applied Optics*, **46**, no. 15, 2922-2929, 2007.
- [5] John E. Barnes, Sebastian Bronner, Robert Beck, and N. C. Parikh, "Boundary Layer Scattering Measurements with a Charge-Coupled Device Camera Lidar", *Applied Optics*, **42**, no. 15, 2647-2652, 2003.
- [6] Nimmi C. P. Sharma and John E. Barnes, "Boundary Layer Characteristics over a High Altitude Station, Mauna Loa Observatory", *Aerosol and Air Quality Research*, **16**, No. 3, 729-737, 2016
- [7] MSIS model access: <https://kauai.ccmc.gsfc.nasa.gov/instantrun/msis>
- [8] AERONET data access: https://aeronet.gsfc.nasa.gov/new_web/index.html
- [9] NASA MERRA2 data access: <https://giovanni.gsfc.nasa.gov/giovanni/>